

One-loop electroweak radiative corrections to lepton pair production in polarized electron-positron collisions

S. Bondarenko*

Bogoliubov Laboratory of Theoretical Physics, JINR, Dubna, 141980 Russia

Ya. Dydyshka,[†] L. Kalinovskaya, R. Sadykov, and V. Yermolchuk[†]
Dzhelepov Laboratory of Nuclear Problems, JINR, Dubna, 141980 Russia

(Dated: May 12, 2020)

This paper presents the high-precision theoretical predictions for $e^+e^- \rightarrow l^-l^+$ scattering. Calculations are performed using the **SANC** system. They take into account complete one-loop electroweak radiative corrections as well as longitudinal polarization of initial beams. Reaction observables are obtained using the helicity amplitude method with taking into account initial and final state fermion masses. Numerical results are given for the center-of-mass energy range $\sqrt{s} = 250 - 1000$ GeV with various degrees of polarization.

I. INTRODUCTION

Planned experiments (with/without polarization of the initial beams) in high energy physics for electron-positron annihilation have been proposed with the capability of precise measurement, such as the International Linear Collider(ILC) [1–6], the e^+e^- Future Circular Collider (FCC-ee) [7–11], the Compact Linear Collider (CLIC) [12–14], and the Circular Electron Positron Collider (CEPC) [15].

The theoretical accuracy for the future e^+e^- colliders should be better than 0.5% [34]. A first calculation of the corrections to the $e^+e^- \rightarrow \mu^-\mu^+$ process was done by Passarino and Veltman [16]. Most of the theoretical works on lepton pair production (LPP) have been concerned with next-to-leading order (NLO) electroweak (EW) radiative corrections (RCs) (see e.g. [17],[18], [19], [20], [21],[22]) before the LEP era.

They were the development of basic codes incorporated to the standard LEP tools such as **TOPAZO** [23], **ZFITTER** [24], and **ALIBABA** [25],[26]. A comprehensive review of the underlying theory and methods which have been used to create these codes can be found in the monograph [27].

Polarized electron/positron beams are important to achieve the relative uncertainty of a few per mille for measurements of the total cross section and left-right asymmetry. In the LEP era results were presented for the theoretical support of the polarized e^+e^- annihilation, see [28], [29],[30],[31],[32],[22],[33]. However, the mentioned investigations have not created a tool at the same level accuracy for the polarized beams.

There are three main e^+e^- processes intended to be used for the high-precision luminometry propose at flavour factories and future colliders: Bhabha, lepton pair production $e^+e^- \rightarrow l^-l^+$ (LPP) and photon pair production $e^+e^- \rightarrow \gamma\gamma$ (PPP).

In the series of papers ([35], [36]) and this paper we recall the above-mentioned three processes taking into account the one-loop EW RC and longitudinally polarized e^+e^- initial beams.

At the moment the most modern and widely used generators **BABAYAGA** [37–39] and **KKMC** [40, 41] with one-loop RCs for these three processes, however, do not support the polarization of the initial beams.

For the unpolarized case we have already presented a comprehensive comparison of the $e^+e^- \rightarrow f\bar{f}$ process with the results of **ZFITTER** for all the light fermion production channels in [42]. In this work we report a brief description of the calculation of the electroweak radiative corrections for the lepton (muon) pair production focusing on the high energy region, including contributions of the longitudinal polarization of the initial states.

In the special case of LPP $e^+e^- \rightarrow \tau^-\tau^+$ reaction the decays of the τ lepton can be used to determine their polarization, which gives extra information on the $Z\tau\tau$ vertex. The polarization effects in this channel will be given in another paper.

In the future e^+e^- collider program the optimized accelerator parameters are: the center-of-mass (c.m.) energy 250 GeV and higher and longitudinal electron $\pm 80\%$ and positron $0, \pm 30\%$ degree of polarization. Moreover it proposes a balance between the polarization and the c.m. energy sets for optimal physics diversity.

In this study the relevant contributions to the cross section are calculated analytically using the helicity amplitudes approach, which allows one to evaluate the contribution of any polarization, and then obtain numerical result. For the first time, the helicity amplitudes were used not only for the Born-like parts but also for the hard photon bremsstrahlung contribution taking into account the initial and final masses of the radiated particles. The effect of polarization of the initial beams is carefully analyzed for certain states. The angular and energy dependence are also considered.

There are many papers devoted to study of the $e^+e^- \rightarrow \mu^+\mu^-$ channel at the one-loop level with polarized effects in the initial state, see e.g. [29],[30] and references

* bondarenko@jinr.ru

[†] Also at Institute for Nuclear Problems, Belarusian State University, Minsk, 220006 Belarus

therein. It is highly non-trivial to perform a tuned comparison of the numerical results, since the authors not always present a complete list of input parameters.

We have performed the high-precision tests at the tree level using the electron-positron branch of the MCSANC integrator [43], [44] and the generator ReneSANCe[45] with the results of alternative codes. The polarized Born and hard photon bremsstrahlung contributions were compared with the corresponding values obtained with the help of the CalcHEP [46] and WHIZARD packages [47–50]. The sum of virtual and soft photon bremsstrahlung contributions in the unpolarized case are compared with the AItalc-1.4 code [51].

The numerical estimations are presented for the total and differential cross sections in the scattering angle $\cos\vartheta_l$, and the relative corrections. Also the left-right asymmetry A_{LR} is given.

The paper is organized as follows. Section II is devoted to the expressions for the covariant (CAs) and helicity amplitudes (HAs) for the Born, virtual and hard photon bremsstrahlung contributions. The approach for the estimation of the polarization effects is also given. Section III contains numerical results for the total and differential cross sections as well as for relative corrections and A_{LR} asymmetry. The comparison with other computer codes are also given. Finally, in Sec. IV we present conclusions and outlook for the further work on LPP process within the SANC framework.

II. DIFFERENTIAL CROSS SECTION

The cross section of the generic process $e^+e^- \rightarrow \dots$ of the longitudinally polarized e^+ and e^- beams with the polarization degrees P_{e^+} and P_{e^-} , can be expressed as follows:

$$\sigma(P_{e^+}, P_{e^-}) = \frac{1}{4} \sum_{\chi_1, \chi_2} (1 + \chi_1 P_{e^+})(1 + \chi_2 P_{e^-}) \sigma_{\chi_1 \chi_2}, \quad (1)$$

where $\chi_{1(2)} = -1(+1)$ correspond to the particle i with the left (right) helicity.

The complete one-loop cross section of the process can be split into four parts:

$$\sigma^{\text{one-loop}} = \sigma^{\text{Born}} + \sigma^{\text{virt}}(\lambda) + \sigma^{\text{soft}}(\lambda, \omega) + \sigma^{\text{hard}}(\omega), \quad (2)$$

where σ^{Born} is the Born cross section, σ^{virt} is the contribution of virtual (loop) corrections, $\sigma^{\text{soft(hard)}}$ is the soft (hard) photon emission contribution (the hard photon energy $E_\gamma > \omega$). Auxiliary parameters λ ("photon mass") and ω are canceled after summation.

We apply the helicity approach to all the contributions.

The virtual (Born) cross section of the $e^+e^- \rightarrow l^-l^+$ process

$$e^+(p_1, \chi_1) + e^-(p_2, \chi_2) \rightarrow l^-(p_3, \chi_3) + l^+(p_4, \chi_4) \quad (3)$$

can be written as follows:

$$\frac{d\sigma_{\chi_1 \chi_2}^{\text{virt(Born)}}}{d \cos \vartheta_l} = \pi \alpha^2 \frac{\beta_l}{8s} |\mathcal{H}_{\chi_1 \chi_2}^{\text{virt(Born)}}|^2, \quad (4)$$

where

$$|\mathcal{H}_{\chi_1 \chi_2}^{\text{virt(Born)}}|^2 = \sum_{\chi_3, \chi_4} |\mathcal{H}_{\chi_1 \chi_2 \chi_3 \chi_4}^{\text{virt(Born)}}|^2, \quad (5)$$

m_l is the final lepton mass and $\beta_l = \sqrt{1 - \frac{4m_l^2}{s}}$, ϑ_l is the angle between the final lepton l^- and initial electron e^- .

The soft photon bremsstrahlung terms (initial state radiation - ISR, interference - IFI, final-state radiation - FSR) are factorized to the Born cross section as follows:

$$\sigma^{\text{soft,ISR}} = -\sigma^{\text{Born}}$$

$$\frac{\alpha}{\pi} Q_e^2 \left\{ (1 + L_e) \ln \left(\frac{4\omega^2}{\lambda} \right) + L_e \left(1 + \frac{1}{2} L_e \right) + \frac{\pi^2}{3} \right\},$$

$$\sigma^{\text{soft,IFI}} = \sigma^{\text{Born}} \frac{\alpha}{\pi} Q_e Q_l \left\{ 2 \ln d_t \ln \left(\frac{4\omega^2}{\lambda} \right) \right.$$

$$\left. + \left[2 \ln \left(1 + \frac{d_t^2}{st} \right) + \ln \left(-\frac{st}{d_t^2} \right) \right] \ln \left(-\frac{st}{d_t^2} \right) \right.$$

$$\left. + \left[2J_l - \ln \left(1 - \frac{2m_l^2}{\beta_l^+ d_t} \right) \right] \ln \left(1 - \frac{2m_l^2}{\beta_l^+ d_t} \right) \right.$$

$$\left. + 2\text{Li}_2 \left(1 + \frac{2t}{\beta_l^+ d_t} \right) - 2\text{Li}_2 \left(-\frac{d_t^2}{st} \right) \right.$$

$$\left. - 2\text{Li}_2 \left(\frac{\beta_l^- d_t}{(m_l^2 + t) - \beta_l d_t} \right) \right\} - \left\{ t \leftrightarrow u \right\},$$

$$\sigma^{\text{soft,FSR}} = -\sigma^{\text{Born}}$$

$$\frac{\alpha}{\pi} Q_l^2 \frac{1}{\beta_l} \left\{ \left[1 + \left(1 - \frac{2m_l^2}{s} \right) J_l \right] \ln \left(\frac{4\omega^2}{\lambda} \right) + J_l \right.$$

$$\left. + \left(1 - \frac{2m_l^2}{s} \right) \left[\frac{1}{2} J_l^2 + 2 \ln \left(-\frac{2\beta}{\beta_l^+} \right) J_l \right. \right.$$

$$\left. \left. + 2\text{Li}_2 \left(\frac{\beta_l^-}{\beta_l^+} \right) + \frac{\pi^2}{3} \right] \right\},$$

where $L_e = \ln(m_e^2/s)$, $\beta_l^\pm = 1 \pm \beta_l$, $J_l = \ln(\beta_l^-)/\beta_l^+$, $d_I = m_l^2 - I$, $I = t, u$.

The cross section for the hard photon bremsstrahlung $e^+(p_1, \chi_1) + e^-(p_2, \chi_2) = l^-(p_3, \chi_3) + l^+(p_4, \chi_4) + \gamma(p_5, \chi_5)$.

is given by the expression

$$\frac{d\sigma_{\chi_1 \chi_2}^{\text{hard}}}{ds' d \cos \theta_4 d\phi_4 d \cos \theta_5} = \alpha^3 \frac{s - s'}{128\pi s^2} \frac{\beta_l'}{\beta_e} |\mathcal{H}_{\chi_1 \chi_2}^{\text{hard}}|^2, \quad (7)$$

where $s' = (p_3 + p_4)^2$, $\beta_l' = \sqrt{1 - 4m_l^2/s'}$ and

$$|\mathcal{H}_{\chi_1 \chi_2}^{\text{hard}}|^2 = \sum_{\chi_3, \chi_4, \chi_5} |\mathcal{H}_{\chi_1 \chi_2 \chi_3 \chi_4 \chi_5}^{\text{hard}}|^2. \quad (8)$$

Here θ_5 is the angle between 3-momenta of the photon and positron, θ_4 is the angle between 3-momenta of the anti-muon μ^+ and photon in the rest frame of (l^-l^+) -compound, ϕ_4 is the azimuthal angle of the μ^+ in the rest frame of (l^-l^+) -compound.

A. Covariant amplitude for Born and virtual part

The covariant one-loop amplitude (CA) corresponds to the result of the straightforward standard calculation by means of SANC programs and procedures of *all* diagrams contributing to the given process at the tree (Born) and one-loop levels. It is represented in a certain basis, made of strings of Dirac matrices and/or external momenta (structures), contracted with polarization vectors of gauge bosons, if any. The amplitude also contains kinematic factors and coupling constants and is parametrized by a certain number of form factors (FF), which we denote by \mathcal{F} , in general with an index labeling the corresponding structure. The number of FFs is equal to the number of structures.

For the processes with non zero tree-level amplitudes the FFs have the form

$$\mathcal{F} = 1 + k\tilde{\mathcal{F}}, \quad (9)$$

where “1” is due to the Born level and the term $\tilde{\mathcal{F}}$ with the factor $k = g^2/16\pi^2$ is due to the one-loop level. After squaring the amplitude we neglect terms proportional to k^2 .

Neglecting the masses of the initial particles the covariant one-loop amplitude of the $e^+e^- \rightarrow l^-l^+$ process can be parametrized by six FFs. If the initial-state masses were not ignored, we would have ten structures with ten scalar form factors and ten independent helicity amplitudes.

We work in the so-called *LQD* basis, which naturally arises if the final-state fermion masses are not ignored. Six form factors $\mathcal{F}_{LL,QL,LQ,QQ,LD,QD}(s,t,u)$, correspond to six Dirac structures. They are labeled according to their structures. A common expression for this CA in terms of \mathcal{F}_{ij} was presented in [42]. We recall it here to introduce the notations. \mathcal{A}_γ is also described by a *QQ* structure, it is separated out for convenience

$$\begin{aligned} \mathcal{A}_\gamma(s) &= i e^2 \frac{Q_e Q_l}{s} \text{Str}_{QQ} \mathcal{F}_\gamma, \\ \mathcal{A}_Z(s) &= i e^2 \frac{\chi_Z(s)}{s} \\ &\left[I_e^{(3)} \left(I_l^{(3)} \text{Str}_{LL} \mathcal{F}_{LL} + \delta_l \text{Str}_{LQ} \mathcal{F}_{LQ} \right) \right. \\ &+ \delta_e \left(I_l^{(3)} \text{Str}_{QL} \mathcal{F}_{QL} + \delta_l \text{Str}_{QQ} \mathcal{F}_{QQ} \right) \\ &\left. + I_l^{(3)} \left(I_e^{(3)} \text{Str}_{LD} \mathcal{F}_{LD} + \delta_e \text{Str}_{QD} \mathcal{F}_{QD} \right) \right]. \end{aligned} \quad (10)$$

We use the following notations for the structures

$$\begin{aligned} \text{Str}_{LL} &= \gamma_\mu (1 + \gamma_5) \otimes \gamma_\mu (1 + \gamma_5), \\ \text{Str}_{QL} &= \gamma_\mu \otimes \gamma_\mu (1 + \gamma_5), \\ \text{Str}_{LQ} &= \gamma_\mu (1 + \gamma_5) \otimes \gamma_\mu, \\ \text{Str}_{QQ} &= \gamma_\mu \otimes \gamma_\mu, \\ \text{Str}_{LD} &= \gamma_\mu (1 + \gamma_5) \otimes (-im_l D_\mu), \\ \text{Str}_{QD} &= \gamma_\mu \otimes (-im_l D_\mu), \end{aligned}$$

where the symbol $\gamma_\mu \otimes \gamma_\mu$ denotes the short-hand notations

$$\gamma_\mu \otimes \gamma_\nu = \bar{v}(p_1) \gamma_\mu u(p_2) \bar{u}(p_3) \gamma_\nu v(p_4), \quad (11)$$

and

$$D_\mu = (p_4 - p_3)_\mu. \quad (12)$$

Here and below $\chi_Z(s)$ is the Z/γ propagator ratio:

$$\chi_Z(s) = \frac{1}{4s_W^2 c_W^2} \frac{s}{s - M_Z^2 + iM_Z \Gamma_Z}. \quad (13)$$

We also use coupling constants

$$\begin{aligned} Q_f, \quad I_f^{(3)}, \quad \sigma_f = v_f + a_f, \quad \delta_f = v_f - a_f, \\ s_W = \frac{e}{g}, \quad c_W = \frac{M_W}{M_Z}. \end{aligned}$$

For more details see [42].

B. Helicity amplitude for virtual part

As was stated we have six non-vanishing HAs. They depend on kinematic variables, coupling constants and six scalar form factors:

$$\begin{aligned} \mathcal{H}_{-+++} &= -c_+ (Q_e Q_l \mathcal{F}_\gamma \\ &+ \chi_Z(s) \delta_e [\beta^- I_l^{(3)} \mathcal{F}_{QL} + \delta_l \mathcal{F}_{QQ}]), \\ \mathcal{H}_{-+ \pm \pm} &= \frac{2m_l}{\sqrt{s}} \sin \vartheta_l (Q_e Q_l \mathcal{F}_\gamma \\ &+ \chi_Z(s) \delta_e [I_l^{(3)} \mathcal{F}_{QL} + \delta_l \mathcal{F}_{QQ} + \frac{s}{2} \beta_l^2 I_l^{(3)} \mathcal{F}_{QD}]), \\ \mathcal{H}_{+- \pm \pm} &= -\frac{2m_l}{\sqrt{s}} \sin \vartheta_l (Q_e Q_l \mathcal{F}_\gamma \\ &+ \chi_Z(s) [2I_e^{(3)} (I_l^{(3)} \mathcal{F}_{LL} + \delta_l \mathcal{F}_{LQ}) + \delta_e I_l^{(3)} \mathcal{F}_{QL} \\ &+ \delta_e \delta_l \mathcal{F}_{QQ} + \frac{s}{2} \beta_f^2 I_l^{(3)} (2I_e^{(3)} \mathcal{F}_{LD} + \delta_e \mathcal{F}_{QD})]), \\ \mathcal{H}_{+---} &= -c_+ (Q_e Q_l \mathcal{F}_\gamma \\ &+ \chi_Z(s) [\beta^+ I_l^{(3)} (2I_e^{(3)} \mathcal{F}_{LL} + \delta_e \mathcal{F}_{QL}) \\ &+ \delta_l (2I_e^{(3)} \mathcal{F}_{LQ} + \delta_e \mathcal{F}_{QQ})]). \end{aligned}$$

The expression for the amplitude \mathcal{H}_{-+++} (\mathcal{H}_{+---}) can be obtained from the expression for $\mathcal{H}_{-+ \pm \pm}$ ($\mathcal{H}_{+- \pm \pm}$) by replacing $c_+ \rightarrow c_-$, $\beta^- \rightarrow \beta^+$.

Helicity indices denote the signs of the fermion spin projections to their momenta p_1, p_2, p_3, p_4 , respectively.

Where,

$$\beta_l^\pm = 1 \pm \beta_l, \quad c_\pm = 1 \pm \cos \vartheta_l,$$

and the scattering angle ϑ_l is related to the Mandelstam invariants t, u :

$$t = m_l^2 - \frac{s}{2}(1 - \beta_l \cos \vartheta_l),$$

$$u = m_l^2 - \frac{s}{2}(1 + \beta_l \cos \vartheta_l).$$

C. Helicity amplitudes for hard photon bremsstrahlung

We present the HAs for $e^+e^-l^+l^-\gamma \rightarrow 0$ ($p_1 + p_2 + p_3 + p_4 + p_5 = 0$) process at any s, t or u channel, where 0 stands for *vacuum*, and all masses are not neglected.

We project all the massive momenta with $p_i^2 = m_i^2$ to the light-cone of photon p_5 and introduce associated ‘‘momenta’’ (auxiliary massless momenta)

$$k_i = p_i - \frac{m_i^2}{2p_i \cdot p_5} p_5 = p_i - \frac{m_i^2}{2k_i \cdot k_5} k_5,$$

$$k_i^2 = k_5^2 = 0, \quad \text{with } i = 1, 2, 3, 4.$$

$$k_5 = - \sum_{i=1}^4 k_i = K p_5,$$

$$K = 1 + \sum_{i=1}^4 \frac{m_i^2}{2p_i \cdot p_5} = 1 + \sum_{i=1}^4 \frac{m_i^2}{2k_i \cdot p_5},$$

$$p_5 = - \sum_{i=1}^4 p_i = K' k_5,$$

$$K' = 1 - \sum_{i=1}^4 \frac{m_i^2}{2p_i \cdot k_5} = 1 - \sum_{i=1}^4 \frac{m_i^2}{2k_i \cdot k_5}.$$

The vector k_5 appears to be light-like, so we are left with ‘‘momentum conservation’’ of associated vectors. The freedom in the light-cone projection choice corresponds to the arbitrariness of the spin quantization direction. We exploit it to make expressions compact.

It is convenient to introduce the following notations

$$\mathcal{D}_I^{ij} = \frac{Q_e Q_l}{I} + \frac{g_e^i g_l^j}{I - M_Z^2 + M_Z \Gamma_Z},$$

where $I = s, s', i = L, R$ and $j = L, R$.

For massless particle with the light-like momentum k_i we use the following notations and relations for spinors

$$|i\rangle = u(k_i, +) = v(k_i, -), \quad [i] = \bar{u}(k_i, +) = \bar{v}(k_i, -),$$

$$|\bar{i}\rangle = u(k_i, -) = v(k_i, +), \quad \langle \bar{i}| = \bar{u}(k_i, -) = \bar{v}(k_i, +),$$

$$\langle i | j \rangle = \langle k_i | k_j \rangle, \quad [j | i] = [k_j | k_i],$$

$$\langle i | j \rangle = -\langle j | i \rangle, \quad [j | i] = -[i | j],$$

$$\langle i | i \rangle = 0, \quad [i | i] = 0, \quad [j | i] = \overline{\langle i | j \rangle}.$$

All non-vanishing amplitudes are obtained from four amplitudes by using CP and cross symmetries

$$A^e_{----++} =$$

$$-\frac{m_e \langle 4 | 5 \rangle [1 | 2]}{K' [1 | 5] [2 | 5]} \left(\frac{[2 | 3]}{\langle 1 | 5 \rangle} \mathcal{D}_{s'}^{LR} + \frac{[1 | 3]}{\langle 2 | 5 \rangle} \mathcal{D}_{s'}^{RR} \right),$$

$$A^e_{-+---+} =$$

$$-\frac{m_l \langle 5 | 2 | 1 \rangle}{K' [1 | 5] [2 | 5]} \left(\frac{[4 | 1]}{\langle 3 | 5 \rangle} \mathcal{D}_{s'}^{RL} + \frac{[3 | 1]}{\langle 4 | 5 \rangle} \mathcal{D}_{s'}^{RR} \right),$$

$$A^e_{-+-++-} =$$

$$-\frac{1}{[2 | 5]} \left[\frac{m_e^2 [1 | 2] [3 | 5 | 4]}{[2 | 5] s_{51}} \mathcal{D}_{s'}^{LR} + \frac{m_l^2 \langle 5 | 2 | 1 \rangle}{K' [3 | 5] [4 | 5]} \mathcal{D}_{s'}^{RL} \right.$$

$$\left. + \frac{[1 | 3]}{[1 | 5]} \left(\frac{\langle 4 | 2 | 1 \rangle}{K'} + \langle 4 | 5 | 1 \rangle \right) \mathcal{D}_{s'}^{RR} \right],$$

$$A^e_{++----} =$$

$$-m_e m_l \langle 1 | 2 \rangle \left(\frac{1}{s_{52}} \left[\frac{[4 | 5]}{\langle 3 | 5 \rangle} \mathcal{D}_{s'}^{LL} + \frac{[3 | 5]}{\langle 4 | 5 \rangle} \mathcal{D}_{s'}^{LR} \right] \right.$$

$$\left. + \frac{1}{s_{51}} \left[\frac{[4 | 5]}{\langle 3 | 5 \rangle} \mathcal{D}_{s'}^{RL} + \frac{[3 | 5]}{\langle 4 | 5 \rangle} \mathcal{D}_{s'}^{RR} \right] \right),$$

where

$$s_{ij} = (p_i + p_j)^2. \quad (14)$$

Using the cross symmetry we can get the lepton radiation amplitudes A^l from the electron radiation radiation amplitudes A^e in the following way

$$A^l_{\chi_1 \chi_2 \chi_3 \chi_4 \chi_5}(p_1, p_2, p_3, p_4, p_5) =$$

$$A^e_{\chi_4 \chi_3 \chi_2 \chi_1 \chi_5}(p_4, p_3, p_2, p_1, p_5) \text{ and } m_e \leftrightarrow m_l.$$

To obtain HA \mathcal{H} with definite helicity, the spin-rotation matrices $C_{\xi_i}^{\chi_i}$ should be applied for each index χ of external particles independently:

$$\mathcal{H}_{\dots \xi_i \dots} = 2\sqrt{2} C_{\xi_1}^{\chi_1} \dots C_{\xi_4}^{\chi_4} (Q_e A^e_{\dots \chi_i \dots} + Q_l A^l_{\dots \chi_i \dots}).$$

$$C_{\xi_i}^{\chi_i} = \begin{bmatrix} \frac{[i^b | 5]}{[i | 5]} & \frac{m_i \langle i^* | 5 \rangle}{\langle i^* | i^b \rangle \langle i | 5 \rangle} \\ \frac{m_i [i^* | 5]}{[i^* | i^b] [i | 5]} & \frac{\langle i^b | 5 \rangle}{\langle i | 5 \rangle} \end{bmatrix} \quad (15)$$

$$= \begin{bmatrix} \frac{\langle i^* | i \rangle}{\langle i^* | i^b \rangle} & \frac{m_i \langle i^* | 5 \rangle}{\langle i^* | i^b \rangle \langle i | 5 \rangle} \\ \frac{m_i [i^* | 5]}{[i^* | i^b] [i | 5]} & \frac{[i^* | i]}{[i^* | i^b]} \end{bmatrix}.$$

$$i = p_i = \{E_i, p_i^x, p_i^y, p_i^z\}, \quad p_i^2 = m_i^2,$$

$$i^* = k_{i^*} = \{|\vec{p}_i|, -p_i^x, -p_i^y, -p_i^z\}, \quad k_{i^*}^2 = 0,$$

$$i^b = k_{i^b} = p_i - \frac{m_i^2}{2p_i \cdot k_{i^*}} k_{i^*}, \quad k_{i^b}^2 = 0. \quad (16)$$

The CP symmetry allows one to obtain the flipped-helicity amplitudes

$$\mathcal{H}_{\chi_1 \chi_2 \chi_3 \chi_4 -} = -\chi_1 \chi_2 \chi_3 \chi_4 \overline{\mathcal{H}}_{-\chi_1 - \chi_2 - \chi_3 - \chi_4 +}$$

with $L \leftrightarrow R$ in \mathcal{D} .

III. NUMERICAL RESULTS AND COMPARISONS

In this section, we show numerical results for EW RC to $e^+e^- \rightarrow \mu^-\mu^+$ scattering obtained by means of the **SANC** system. Comparison of our results for specific contributions at the tree level with **CalcHEP** [46] and **WHIZARD** [47–50] are given. The numerical results are completed with the estimation of the polarized effect and evaluation of angular and energy distributions at the one-loop level.

We used the following set of the input parameters

$$\alpha^{-1}(0) = 137.03599976, \quad (17)$$

$$\begin{aligned} M_W &= 80.45150 \text{ GeV}, & M_Z &= 91.1867 \text{ GeV}, \\ \Gamma_Z &= 2.49977 \text{ GeV}, & m_e &= 0.51099907 \text{ MeV}, \\ m_\mu &= 0.105658389 \text{ GeV}, & m_\tau &= 1.77705 \text{ GeV}, \\ m_d &= 0.083 \text{ GeV}, & m_s &= 0.215 \text{ GeV}, \\ m_b &= 4.7 \text{ GeV}, & m_u &= 0.062 \text{ GeV}, \\ m_c &= 1.5 \text{ GeV}, & m_t &= 173.8 \text{ GeV}. \end{aligned}$$

The $\alpha(0)$ and G_μ EW schemes are used in calculations. All the results are obtained for the c.m. energies $\sqrt{s} = 250, 500$ and 1000 GeV and for the following magnitudes of the electron (P_{e^-}) and the positron (P_{e^+}) beam polarizations:

$$(P_{e^-}, P_{e^+}) = (0, 0), (-0.8, 0), (-0.8, 0.3), (0.8, 0), (0.8, -0.3). \quad (18)$$

A. The comparison with another codes

1. The triple comparison of Born and hard photon bremsstrahlung cross sections

First of all we compared the numerical results for the polarized Born and hard photon bremsstrahlung cross section with the ones obtained with the help of the **CalcHEP** and **WHIZARD**. The agreement for the Born cross section was found to be excellent.

In the Table I the triple tuned comparison between the **SANC** (S) and the **CalcHEP** (C) and **WHIZARD** (W) of the hard photon bremsstrahlung (6) cross section calculations are given.

The results are given within the $\alpha(0)$ scheme for c.m. energies $\sqrt{s} = 250, 500$ and 1000 GeV, $\omega = 10^{-4}$, and the fixed 100% polarized initial states in the total phase space.

The comparison demonstrates a very good (within 4-5 digits) agreement with the above-mentioned codes.

2. Comparison of virtual and soft photon bremsstrahlung contributions

We have obtained a very good agreement (six significant digits) in the comparison of the **SANC** and

P_{e^-}, P_{e^+}	-1, -1	1, -1	-1, 1	1, 1
	$\sigma_{e^+e^-}^{\text{hard}}, \text{ fb}, \sqrt{s} = 250, \text{ GeV}$			
S	169.0(1)	8802(1)	11263(1)	169.0(1)
C	169.8(1)	8824(2)	11294(2)	169.8(1)
W	167.3(1)	8802(1)	11261(2)	168.4(1)
	$\sigma_{e^+e^-}^{\text{hard}}, \text{ fb}, \sqrt{s} = 500, \text{ GeV}$			
S	47.38(1)	2314(1)	2899(1)	47.38(1)
C	47.63(3)	2318(1)	2905(1)	47.55(4)
W	46.81(1)	2313(1)	2900(1)	46.94(1)
	$\sigma_{e^+e^-}^{\text{hard}}, \text{ fb}, \sqrt{s} = 1000, \text{ GeV}$			
S	12.65(1)	624.7(1)	778.8(1)	12.65(1)
C	12.70(1)	626.1(1)	780.3(2)	12.70(1)
W	12.48(2)	624.7(1)	778.8(1)	12.54(1)

TABLE I. The triple tuned comparison between the **SANC** (S) and the **CalcHEP** (C) and **WHIZARD** (W) of the hard photon bremsstrahlung (6) cross section calculations.

AIitalc-1.4 [51] results for the unpolarized differential Born cross section and for the sum of the virtual and the soft photon bremsstrahlung contributions. The comparison was done for the different values of the scattering angles ($\cos\vartheta$: from -0.9 up to $+0.9999$).

B. The Born, one-loop cross sections and relative corrections

1. The energy dependence

In Tables II - IV the results of the Born cross sections, weak contribution (weak) and complete one-loop contributions (EW) as well as the relative corrections δ (%) for the c.m. energies $\sqrt{s} = 250, 500, 1000$ GeV and the set (18) of the polarization degree of the initial particles in the $\alpha(0)$ and G_μ EW schemes are presented. The results were obtained without any angular cuts.

The relative corrections δ (in %) is defined as

$$\delta = \frac{\sigma^{\text{one-loop}}(P_{e^-}, P_{e^+})}{\sigma^{\text{Born}}(P_{e^-}, P_{e^+})} - 1. \quad (19)$$

As it seen from the tables the corrections for all considered c.m. energies, EW-schemes and degrees of polarization are positive rather large and equal to about 170-175% for the c.m energy $\sqrt{s} = 250$ GeV, about 182-186% for the c.m energy $\sqrt{s} = 500$ GeV and about 200-204% for the c.m energy $\sqrt{s} = 1000$ GeV in $\alpha(0)$ EW-scheme. The calculations in the G_μ scheme reduce the RCs to the about 5-6 %.

The main impact to the one-loop corrections is due to the QED contributions. It can be described by large logarithms of the radiating particle masses ($\ln s/m_l^2$) appeared for the collinear photons. The contribution of the collinear photons is clearly seen from Fig. 1 where the rapid increasing of the cross section at small angles of final muon ($|\cos\vartheta_\mu| \approx 1$) is observed. The real-life experimental angular cuts can rapidly reduce the QED radiative corrections and the whole cross section.

TABLE II. Born cross sections, weak contribution (weak) and complete one-loop contributions (EW), and relative corrections δ (%) for the c.m. energy $\sqrt{s} = 250$ GeV and the set (18) of the polarization degree of the initial particles in the $\alpha(0)$ and G_μ EW schemes.

P_{e^+}, P_{e^-}	0, 0	0,-0.8	0.3,-0.8	0,0.8	-0.3,0.8
$\sigma_{\alpha(0)}^{\text{Born}}$, pb	1.6537(1)	1.8040(1)	2.2572(1)	1.5034(1)	1.8440(1)
$\sigma_{G_\mu}^{\text{Born}}$, pb	1.7611(1)	1.9212(1)	2.4039(1)	1.6011(1)	1.9638(1)
$\sigma_{\alpha(0)}^{\text{weak}}$, pb	1.8360(1)	1.9447(1)	2.4261(1)	1.7273(1)	2.1271(1)
δ , %	11.03(1)	7.81(1)	7.49(1)	14.89(1)	15.36(1)
$\sigma_{G_\mu}^{\text{weak}}$, pb	1.8547(1)	1.9614(1)	2.4466(1)	1.7480(1)	2.1532(1)
δ , %	5.31(1)	2.10(1)	1.78(1)	9.18(1)	9.64(1)
$\sigma_{\alpha(0)}^{\text{EW}}$, pb	4.534(1)	4.923(1)	6.115(1)	4.145(1)	5.047(1)
δ , %	174.2(1)	172.9(1)	170.9(1)	175.7(1)	173.7(1)
$\sigma_{G_\mu}^{\text{EW}}$, pb	4.728(1)	5.132(1)	6.376(1)	4.323(1)	5.263(1)
δ , %	168.5(1)	167.1(1)	165.2(1)	170.0(1)	168.0(1)

The degree of the initial particles polarization changes the magnitude of the cross section, the minimal value achieved for unpolarized beams and the maximum (from the set 18) for the $(P_{e^-}, P_{e^+}) = (0.3, -0.8)$ ones. It can be useful to increase the signal reaction.

2. The angular distributions

In Fig. 1 the dependence of the muon angle of emission is shown for the unpolarized Born and complete one-loop cross section for c.m. energies $\sqrt{s} = 250, 500$ and 1000 GeV. As it seen the Born distributions are rather smooth while the EW one-loop RCs have large values at the small angles. As it was mentioned above, this is due to the collinear emitted photons. Both distributions are asymmetric.

Since the polarization effects do not change the form of the distributions, the only unpolarized cross section is shown. The integrated values of the polarization effects are shown in the Tables. II - IV.

C. The left-right asymmetry

In Fig. 2 the left-right asymmetry distributions are shown as a function of the muon angle cosine. The A_{LR} is defined in the following form

$$A_{LR} = \frac{\sigma_{LR} - \sigma_{RL}}{\sigma_{LR} + \sigma_{RL}}, \quad (20)$$

where σ_{LR} and σ_{RL} are the cross sections for 100% polarized electron-positron $e_L^- e_R^+$ and $e_R^- e_L^+$ initial states.

The A_{LR} asymmetry distributions for the Born and one-loop contribution are shown for three c.m. energies $\sqrt{s} = 250, 500, 1000$ GeV.

One sees that the EW RCs affect very strongly to the asymmetry. The Born contribution to A_{LR} has smooth dependance on the $\cos \vartheta_\mu$ and equals to zero at $\cos \vartheta_\mu =$

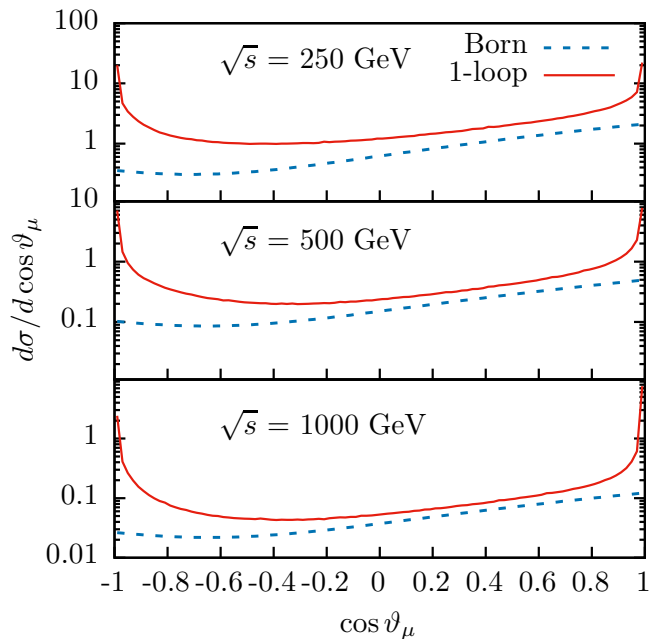


FIG. 1. The Born (dashed line) and one-loop (solid line) differential cross sections of the $e^+e^- \rightarrow \mu^-\mu^+$ reaction for the c.m. energies $\sqrt{s} = 250, 500, 1000$ GeV.

-1 and to the value $0.12 - 0.14$ depending on the c.m. energy. The one-loop contribution has two maxima: first at $\cos \vartheta_\mu = 1$ and another one at $\cos \vartheta_\mu = -0.6$ for $\sqrt{s} = 250$ GeV, $\cos \vartheta_\mu = -0.8$ for $\sqrt{s} = 500$ GeV and around the $\cos \vartheta_\mu = -1$ for $\sqrt{s} = 1000$ GeV.

During the LEP era the A_{LR} asymmetry (as well as the A_{FB} , $A_{FB,LR}$ and final lepton polarization) calculated at the Z pole were used to measure experimentally the $\sin^2 \theta_W$. The comprehensive investigation of the one-loop contribution to the above-mentioned variables will be published elsewhere.

IV. CONCLUSIONS AND OUTLOOK

The theoretical description of the $e^+e^- \rightarrow l^+l^-$ scattering taking into account the complete one-loop and high-order radiative corrections is crucial for the luminosity monitoring at the modern and future e^+e^- colliders. Consideration of the beam polarization is a novel requirement for the theoretical predictions for the e^+e^- collisions at the energies of CLIC and ILC.

In the paper we have described the implementation of the complete one-loop EW calculations including the hard photon bremsstrahlung contribution into the SANC framework. It allows one to calculate the observables for the polarization processes of the lepton pair production.

In this study the relevant contributions to the cross section are calculated analytically using the helicity amplitudes approach, which allows one to evaluate the contribution of any polarization, and then estimated numeri-

TABLE III. The same as in Tab. II for the c.m. energy $\sqrt{s} = 500$ GeV.

P_{e^+}, P_{e^-}	0, 0	0,-0.8	0.3,-0.8	0,0.8	-0.3,0.8
$\sigma_{\alpha(0)}^{\text{Born}}$, pb	0.40084(1)	0.43351(1)	0.54196(1)	0.36820(1)	0.45215(1)
$\sigma_{G_\mu}^{\text{Born}}$, pb	0.42689(1)	0.46167(1)	0.57717(1)	0.39211(1)	0.48152(1)
$\sigma_{\alpha(0)}^{\text{weak}}$, pb	0.44633(1)	0.46766(1)	0.58278(1)	0.42501(1)	0.52413(1)
δ , %	11.35(1)	7.88(1)	7.53(1)	15.43(1)	15.92(1)
$\sigma_{G_\mu}^{\text{weak}}$, pb	0.45095(1)	0.47168(1)	0.58768(1)	0.43022(1)	0.53067(1)
δ , %	5.64(1)	2.17(1)	1.82(1)	9.72(1)	10.21(1)
$\sigma_{\alpha(0)}^{\text{EW}}$, pb	1.145(1)	1.233(1)	1.531(1)	1.056(1)	1.286(1)
δ , %	185.7(1)	184.5(1)	182.4(1)	186.8(1)	184.5(1)
$\sigma_{G_\mu}^{\text{EW}}$, pb	1.195(1)	1.287(1)	1.597(1)	1.102(1)	1.342(1)
δ , %	180.0(1)	178.8(1)	176.7(1)	181.1(1)	178.8(1)

TABLE IV. The same as in Tab. II for the c.m. energy $\sqrt{s} = 1000$ GeV.

P_{e^-}, P_{e^+}	0, 0	0,-0.8	0.3,-0.8	0,0.8	0.8,-0.3
$\sigma_{\alpha(0)}^{\text{Born}}$, pb	0.099570(1)	0.107474(1)	0.134335(1)	0.091666(1)	0.112599(1)
$\sigma_{G_\mu}^{\text{Born}}$, pb	0.106038(1)	0.114455(1)	0.143061(1)	0.097620(1)	0.119913(1)
$\sigma_{\alpha(0)}^{\text{weak}}$, pb	0.11017(1)	0.11422(1)	0.14218(1)	0.10611(1)	0.13103(1)
δ , %	10.64(1)	6.28(1)	5.85(1)	15.8(1)	16.4(1)
$\sigma_{G_\mu}^{\text{weak}}$, pb	0.11127(1)	0.11511(1)	0.14325(1)	0.10743(1)	0.13269(1)
δ , %	4.93(1)	0.57(1)	0.13(1)	10.05(1)	10.66(1)
$\sigma_{\alpha(0)}^{\text{EW}}$, pb	0.3003(1)	0.3223(1)	0.3997(1)	0.2782(1)	0.3392(1)
δ , %	201.6(1)	199.9(1)	197.5(1)	203.5(1)	201.2(1)
$\sigma_{G_\mu}^{\text{EW}}$, pb	0.3137(1)	0.3367(1)	0.4176(1)	0.2907(1)	0.3543(1)
δ , %	195.9(1)	194.2(1)	191.9(1)	197.8(1)	195.5(1)

cally. For the first time the helicity amplitudes were used not only for the Born-like parts but also for the hard photon bremsstrahlung contribution taking into account the initial and final masses of the radiate particles. The effect of polarization of the initial beams is carefully analyzed for certain states. The angular and energy dependencies are also considered.

All contributions to the complete one-loop corrections, i.e. Born, virtual and real soft- and hard photon bremsstrahlung were obtained using the helicity amplitude approach. The independence of the form factors of the gauge parameters was tested, the stability of the result from the variation of the soft-hard separation parameter ω was checked.

The calculated polarized tree-level cross sections for the Born and hard photon bremsstrahlung were compared with the CalCHEP and WHIZARD results and a very good (within 4-5 digits) agreement with the above-mentioned codes was found.

Also we obtained a very good agreement (six significant digits) in the comparison of the SANC and AItalc-1.4 [51] results for the unpolarized differential Born cross section and for the sum of the virtual and the

soft photon bremsstrahlung contributions.

As a result, the polarization effects is significant and gives increase of the cross section at the definite initial degrees of polarization compared to the unpolarized one.

We show that the complete $\mathcal{O}(\alpha)$ electroweak radiative corrections provide a considerable impact on the differential cross section and the left-right asymmetry A_{LR} . Moreover, the corrections themselves are rather sensitive to polarization degrees of the initial beams and depend quite strongly on the energy.

Considering the $e^+e^- \rightarrow l^-l^+$ process as one for luminometry propose, one needs to take into account high-order effects, such as leading multi-photon QED logarithms and mixed QCD-EW multi-loop corrections. These corrections will be implemented in the future.

ACKNOWLEDGMENTS

This work has been supported by the RFBR grant 20-02-00441. We are grateful to Drs. A. Gladyshev and A. Saproinov for the help in the preparation of the manuscript.

[1] “ILC Technical Design Report: Volume 1”, edited by Ties Behnke, James E. Brau, Brian Foster, Juan

Fuster, Mike Harrison, James McEwan Paterson, Michael Peskin, Marcel Stanitzki, Nicholas Walker, Hi-

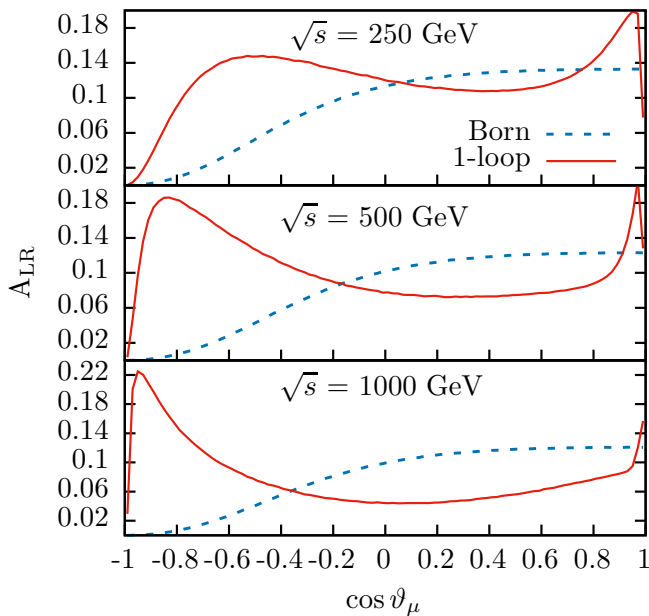


FIG. 2. The A_{LR} asymmetries distribution dependence of the muon angle for Born (dashed line) and one-loop (solid line) contributions for three c.m. energies $\sqrt{s} = 250, 500, 1000$ GeV.

- toshi Yamamoto, 1306.6327; ILC — <https://www.linearcollider.org/ILC>.
- [2] A. Irlles, R. Poschl, F. Richard, and H. Yamamoto, “Complementarity between ILC250 and ILC-GigaZ”, in *Linear Collider Community Meeting Lausanne, Switzerland, April 8-9, 2019*, 2019, 1905.00220.
- [3] A. Arbey *et al.*, *Eur. Phys. J. C* **75** (2015), no. 8 371, 1504.01726.
- [4] H. Baer, T. Barklow, K. Fujii, Y. Gao, A. Hoang, S. Kanemura, J. List, H. E. Logan, A. Nomerotski, M. Perelstein, *et al.*, 1306.6352.
- [5] ECFA/DESY LC Physics Working Group Collaboration, E. Accomando *et al.*, *Phys. Rept.* **299** (1998) 1–78, [hep-ph/9705442](https://arxiv.org/abs/hep-ph/9705442).
- [6] CLIC Physics Working Group Collaboration, E. Accomando *et al.*, “Physics at the CLIC multi-TeV linear collider”, in *Proceedings, 11th International Conference on Hadron spectroscopy (Hadron 2005): Rio de Janeiro, Brazil, August 21-26, 2005*, 2004, [hep-ph/0412251](https://arxiv.org/abs/hep-ph/0412251).
- [7] Abada, A. *et al.*, “FCC-ee: The Lepton Collider: Future Circular Collider Conceptual Design Report Volume 2”, *Eur. Phys. J. ST*, **228**, no. 2, 261-623 (2019); FCC-ee — <http://tlep.web.cern.ch>.
- [8] FCC Collaboration, A. Abada *et al.*, *Eur. Phys. J. ST* **228** (2019), no. 5 1109–1382.
- [9] FCC Collaboration, A. Abada *et al.*, *Eur. Phys. J. C* **79** (2019), no. 6 474.
- [10] A. Blondel and P. Janot, 1912.11871.
- [11] A. Blondel *et al.*, “Standard model theory for the FCC-ee Tera-Z stage”, in *Mini Workshop on Precision EW and QCD Calculations for the FCC Studies: Methods and Techniques CERN, Geneva, Switzerland, January 12-13, 2018*, vol. 3, CERN, CERN, Geneva, 2019, 1809.01830.
- [12] “A Multi-TeV linear collider based on CLIC technology: CLIC Conceptual Design Report”, edited by M. Aicheler, P. Burrows, M. Draper, T. Garvey, P. Lebrun, K. Peach, N. Phinney, H. Schmickler, D. Schulte and N. Toge, CERN-2012-007, SLAC-R-985, KEK-Report-2012-1, PSI-12-01, JAI-2012-001; CLIC — <http://clic-study.web.cern.ch>.
- [13] CLIC, CLICdp Collaboration, M. J. Boland *et al.*, 1608.07537.
- [14] CLICdp, CLIC Collaboration, T. K. Charles *et al.*, *CERN Yellow Rep. Monogr.* **1802** (2018) 1–98, 1812.06018.
- [15] CEPC — <http://cepc.ihep.ac.cn>.
- [16] G. Passarino and M. J. G. Veltman, *Nucl. Phys.* **B160** (1979) 151–207.
- [17] D. Yu. Bardin, P. K. Khristova, and O. M. Fedorenko, *Nucl. Phys.* **B197** (1982) 1–44.
- [18] D. Yu. Bardin, P. K. Khristova, and O. M. Fedorenko, *Nucl. Phys.* **B175** (1980) 435–461.
- [19] A. A. Akhundov, D. Yu. Bardin, O. M. Fedorenko, and T. Riemann, *Sov. J. Nucl. Phys.* **42** (1985) 762, [*Yad. Fiz.*42,1204(1985)].
- [20] F. A. Berends, G. Burgers, W. Hollik, and W. L. van Neerven, *Phys. Lett.* **B203** (1988) 177–182.
- [21] D. Yu. Bardin, M. S. Bilenky, T. Riemann, M. Sachwitz, and H. Vogt, *Comput. Phys. Commun.* **59** (1990) 303–312.
- [22] W. F. L. Hollik, *Fortsch. Phys.* **38** (1990) 165–260.
- [23] G. Montagna, O. Nicrosini, F. Piccinini, and G. Passarino, *Comput. Phys. Commun.* **117** (1999) 278–289, [hep-ph/9804211](https://arxiv.org/abs/hep-ph/9804211).
- [24] D. Yu. Bardin, P. Christova, M. Jack, L. Kalinovskaya, A. Olchevski, S. Riemann, and T. Riemann, *Comput. Phys. Commun.* **133** (2001) 229–395, [hep-ph/9908433](https://arxiv.org/abs/hep-ph/9908433).
- [25] W. Beenakker, F. A. Berends, and S. C. van der Marck, *Nucl. Phys.* **B349** (1991) 323–368.
- [26] W. Beenakker, F. A. Berends, and S. C. van der Marck, *Phys. Lett.* **B251** (1990) 299–304.
- [27] D. Yu. Bardin and G. Passarino, *The standard model in the making: Precision study of the electroweak interactions*. 1999.
- [28] D. Yu. Bardin, O. M. Fedorenko, and N. M. Shumeiko, *Sov. J. Nucl. Phys.* **32** (1980) 403, [*Yad. Fiz.*32,782(1980)].
- [29] W. Hollik, *Z. Phys.* **C8** (1981) 149.
- [30] M. Bohm and W. Hollik, *Nucl. Phys.* **B204** (1982) 45–77.
- [31] M. Bohm and W. Hollik, *Phys. Lett.* **139B** (1984) 213–216.
- [32] T. V. Kukhto and N. M. Shumeiko, *Nucl. Phys.* **B219** (1983) 412–436.
- [33] M. W. Grunewald, *Phys. Rept.* **322** (1999) 125–346.
- [34] A. Blondel, A. Freitas, J. Gluza, T. Riemann, S. Heine-meyer, S. Jadach, and P. Janot, 1901.02648.
- [35] D. Bardin, Y. Dydyshka, L. Kalinovskaya, L. Rumyantsev, A. Arbuzov, R. Sadykov, and S. Bondarenko, *Phys. Rev.* **D98** (2018), no. 1 013001, 1801.00125.
- [36] *to be published*
- [37] C. M. Carloni Calame, *EPJ Web Conf.* **142** (2017) 01006.
- [38] G. Balossini, C. M. Carloni Calame, G. Montagna, O. Nicrosini, and F. Piccinini, *Nucl. Phys. Proc. Suppl.* **162** (2006) 59–62, [,59(2006)], [hep-ph/0610022](https://arxiv.org/abs/hep-ph/0610022).
- [39] C. M. Carloni Calame, G. Montagna, O. Nicrosini, and F. Piccinini, *Nucl. Phys. Proc. Suppl.* **131** (2004) 48–55, [,48(2003)], [hep-ph/0312014](https://arxiv.org/abs/hep-ph/0312014).

- [40] S. Jadach, B. Ward and Z. Was, *Phys. Rev. D* **88** (2013) no.11 114022 [hep-ph/1307.4037](#).
- [41] S. Jadach, B. Ward and Z. Was, *Comput. Phys. Commun.* **130** (2000) 260-325 [hep-ph/9912214](#).
- [42] A. Andonov, D. Bardin, S. Bondarenko, P. Christova, L. Kalinovskaya, and G. Nanava, *Phys. Part. Nucl.* **34** (2003) 577–618, [*Fiz. Elem. Chast. Atom. Yadra*34,1125(2003)], [hep-ph/0207156](#).
- [43] S. G. Bondarenko and A. A. Saproinov, *Comput. Phys. Commun.* **184** (2013) 2343–2350, [1301.3687](#).
- [44] A. Arbuzov, D. Bardin, S. Bondarenko, P. Christova, L. Kalinovskaya, U. Klein, V. Kolesnikov, L. Romyantsev, R. Sadykov, and A. Saproinov, *JETP Lett.* **103** (2016), no. 2 131–136, [1509.03052](#).
- [45] R. Sadykov and V. Yermolchik, [2001.10755](#).
- [46] A. Belyaev, N. D. Christensen, and A. Pukhov, *Comput. Phys. Commun.* **184** (2013) 1729–1769, [1207.6082](#).
- [47] T. Ohl, “WHiZard and O’Mega”, in *Proceedings, LoopFest V: Radiative Corrections for the International Linear Collider: Multi-loops and Multi-legs: SLAC, Menlo Park, California, June 19-21, 2006*, 2006.
- [48] W. Kilian, T. Ohl, and J. Reuter, *Eur. Phys. J.* **C71** (2011) 1742, [0708.4233](#).
- [49] W. Kilian, F. Bach, T. Ohl, and J. Reuter, “WHIZARD 2.2 for Linear Colliders”, in *International Workshop on Future Linear Colliders (LCWS13) Tokyo, Japan, November 11-15, 2013*, 2014, [1403.7433](#).
- [50] W. Kilian, S. Brass, T. Ohl, J. Reuter, V. Rothe, P. Stienemeier, and M. Utsch, “New Developments in WHIZARD Version 2.6”, in *International Workshop on Future Linear Collider (LCWS2017) Strasbourg, France, October 23-27, 2017*, 2018, [1801.08034](#).
- [51] J. Fleischer, J. Gluza, A. Lorca, T. Riemann, *Eur. J. Phys.* **C48**, 35 (2006), [0606210](#) [[hep-ph](#)]